30

# Voltage Stability Analysis of Automotive Power Nets Based on Modeling and Experimental Results

Tom P. Kohler[1], Rainer Gehring[2], Joachim Froeschl[2], Dominik Buecherl[1] and Hans-Georg Herzog[1]
[1]*Technische Universitaet Muenchen*
[2]*BMW Group*
*Germany*

## 1. Introduction

In recent years, there has been a trend toward increasing electrification in automotive engineering. On the one hand, the quantity of electronic control units (ECUs) as well as installed functions has increased. With the goal of reduced fuel consumption, engine-start-stop systems were being introduced, and more and more components which were previously mechanically driven are now electrically operated. In today's luxury class vehicles there are up to 80 ECUs (Polenov et al., 2007; Hillenbrand & Muller-Glaser, 2009) servicing an wider range of customer needs in the areas of comfort, driving dynamics, and safety. On the other hand, the demands for electrical power as well as the power dynamics have permanently been increasing, as well. Loads like electrical power steering, chassis control systems, and engine cooling fans with more than 1 kW peak power are installed in the 12 V power net. Fig. 1 presents the increase of both installed alternator power and the total nominal current of the fuses in the latest decades.

As the electric power demand increases, automotive power nets must operate close to their limits and it has become increasingly difficult to guarantee voltage stability within the 12 V system (Surewaard & Thele, 2005; Gerke & Petsch, 2006; Polenov et al., 2007). In the example of a luxury class vehicle, the continuous power of heating in winter, air conditioning in summer, ECUs, sensors, and consumer electronics can be more than 600 W. If this load is augmented by electric chassis control systems, voltage drops will be inevitable. Voltages below a certain level across the terminals of electrical components can lead to non specified behaviour. This can be manifested in a flicker of lights or changes in noise of the blower fans (Surewaard & Thele, 2005), a malfunction of the navigation system or even an ECU reset. Therefore, such complex problems are not only be noticeable to passengers, but are also a safety relevant issue.

To guarantee the proper functioning of all electrical components, a stable voltage supply must be realized during the development and design of the electrical power net. For this reason, a thorough understanding of the electrical phenomena in distributed power nets is necessary.

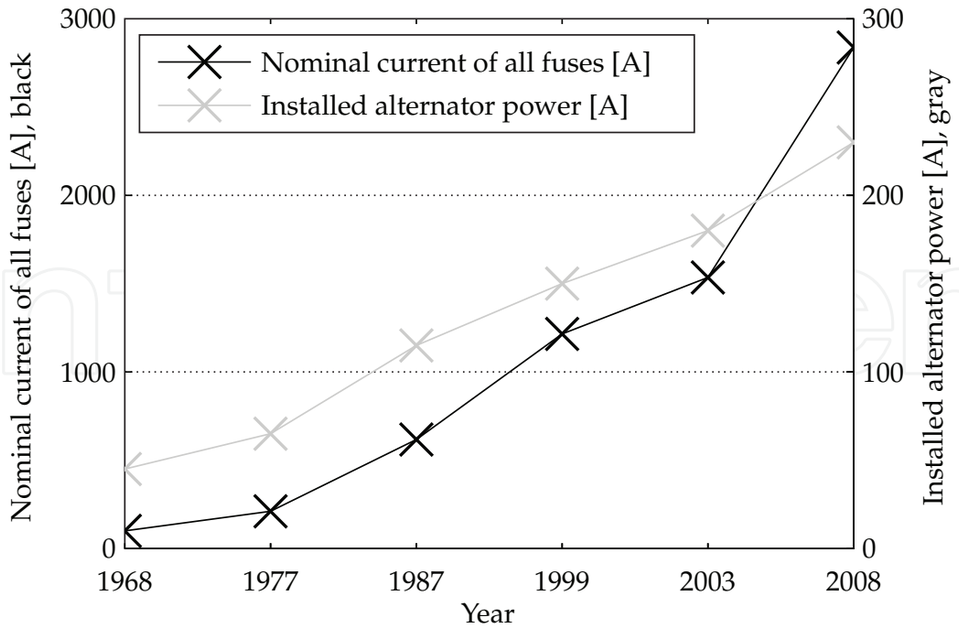


Fig. 1. Increase of the total nominal current of the fuses (left scale) and the installed alternator power (right scale) in the latest decades.

## 2. Goals and approach

This paper describes the modeling of a distributed automotive power net with emphasis on the wiring harness and the chassis ground. All relevant physical effects and electrical phenomena should be taken into account to enable sustainable statements on voltage stability. With this knowledge, a modeling environment will be developed that enables simulations and analysis of the voltage characteristics within the entire wiring harness. So critical situations can be detected, an optimization of both power demand and topology of power nets must be feasible.

First of all, the electric power net and its components are described to give a system understanding. Likewise, a power net test bench is presented, to serve as a platform to verify and evaluate the simulation results. In the next step, the primary components necessary for power net analysis are examined. Besides the alternator, battery, load, and fuses, the focus is on the modeling of the chassis ground as well as the wiring harness.

After deducing characteristic equations of the electrical field, voltage drop, DC resistance, and AC resistance from physical laws, the respective models are compared with measurements of the real components in the power net test bench which was previously introduced.

In the analysis of the chassis ground, a method for calculating the resistance between two grounding bolts is shown. Important technical aspects of the car body are also discussed, such as the thickness of the sheet steel or the influence of the weld seam at the grounding bolts. As part of the development of the wiring harness model, the derivation of the per length parameters $R'$, $L'$, and $C'$ is discussed, and the influence of the existing frequencies is considered. Furthermore, guidelines that show appropriate models for different frequencies are derived. Next, the entire distributed network of the electrical power net of a luxury class vehicle is investigated, and conclusions concerning voltage stability are drawn. Finally, we present an outlook on further research.

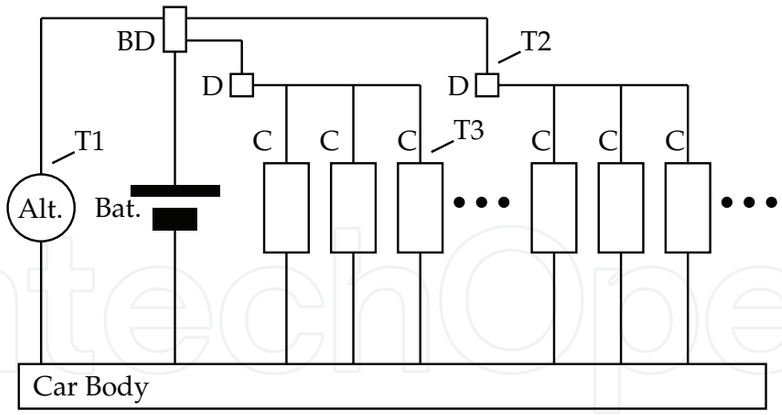


Fig. 2. Schematic of the automotive 12 V power net. The alternator (Alt.) is connected to the battery (Bat.) via the battery distribution unit (BD). The electrical components (C) are supplied via further distribution boxes (D). These are connected to the car body to close the circuits to the alternator and the battery. T1, T2, and T3 are test points of the measurement in Fig. 4.

## 3. The electric power net

The automotive power net serves the electric and electronic components in the vehicle with electric power. In this article, the wiring of the communication systems such as bus lines or sensor and signal wires are not perceived as a part of the electric power net.

### 3.1 Single level power nets

At first, to begin with a basic example, only power nets with one single voltage level are considered. A schematic topology of a 12 V power net is shown in Fig. 2. The alternator (Alt. in Fig. 2), which is coupled via a belt drive to the combustion engine, is used as an energy source. It delivers electrical energy to charge the battery (Bat.) and to supply the electrical components (C).

The alternator is able to supply all power demands and forces the maximum voltage to its setpoint of about 14 V in normal operation. Both at the start-up of the combustion engine and when the power demand of all loads exceeds the alternator's supply, the battery must provide the power difference. In this case, the power net voltage decreases to the battery's terminal voltage of 12.7 V and below (Kiehne, 2003). Due to the internal resistance of the battery, the terminal voltage depends on the battery load, and further voltage reductions occur in case of high current demands. Therefore, the resulting voltage at the battery's terminals can be significantly lower than 12 V. Since the alternator's dynamics are limited in order to avoid fluctuations of the combustion engine speed and reduction of customer's driving comfort (Reif, 2009) these voltage drops occur especially when a significant current draw with a short rising time occurs.

Starting from the battery distribution box (BD), all electrical components (C) are connected to the power net via further distribution boxes (D) and wires that are assembled to a wiring harness. The negative terminals of the components are connected via wires to grounding bolts that are welded to the car body (Fig 3a). The negative terminal of the battery is also connected to a nearby grounding bolt. This means that the car body is used as a return conductor to close the circuits to the battery. Additionally, there are further voltage reductions in the distributed system of the wiring harness, in power distribution units, and in fuse boxes.

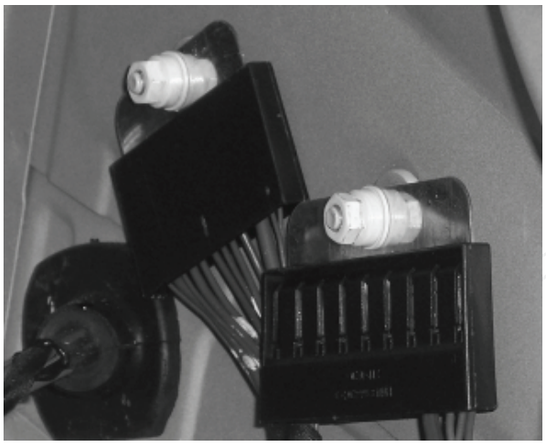

(a) The negative terminals of the components are connected to bus bars. Here, two bus bars are screwed to two grounding bolts that are welded to the car body.

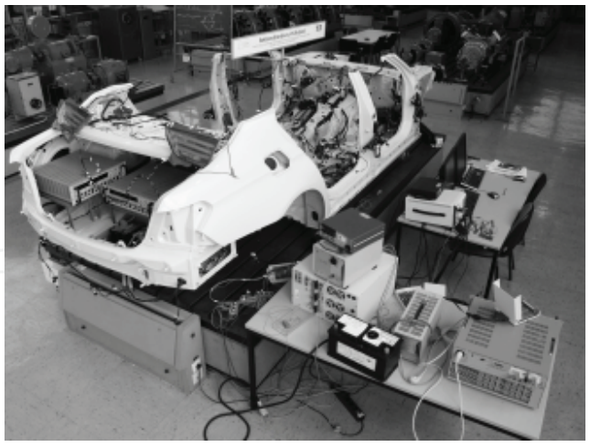

(b) Installation of the power net test bench using an entire power net consisting of an original car body and wiring harness of a luxury class vehicle as well as source, storage and loads.

Fig. 3. Power net test bench.

Therefore, the installation point of a component is an important factor in determining its resulting voltage. Thus, the electric power net can be modelled as a tree with the root node at the positive terminal of the alternator or battery and all end-nodes connected to the car body return conductor.

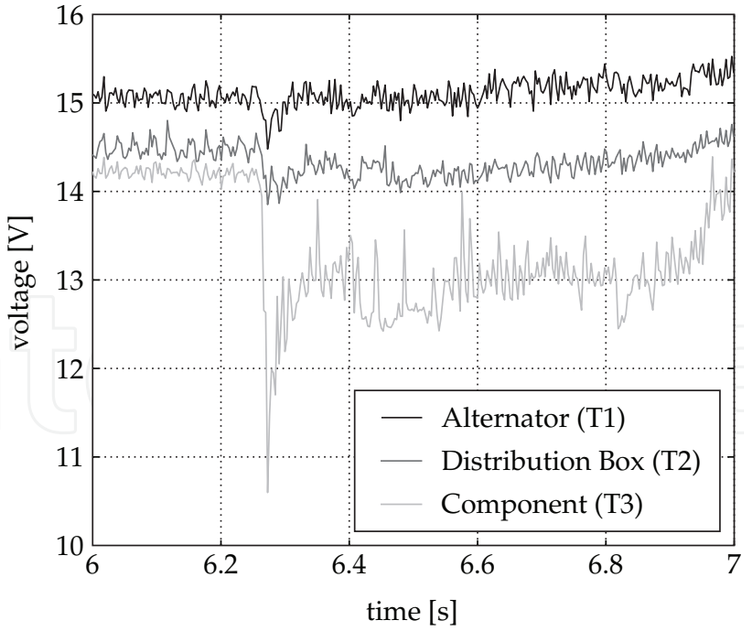


Fig. 4. Voltage curves measured across test points at the alternator (T1), a distribution box (T2), and at the terminals of a chassis control system (T3), see Fig. 2. The different voltage levels and voltage drops show that the voltage at each component depends on its connection to the power net.

The measured voltage curves at a high power demand during the start-up of an electrical chassis control system are exemplified in Fig. 4. The peak current of the chassis control system is 50 A. The current peak of 50 A causes a voltage drop of 3.5 V at the terminals of the chassis control system (test point T3 in Fig. 2). At the distribution box, a drop of 0.7 V can be detected (T2); at the alternator, the voltage drop is 0.6 V (T1).
Thus, it can be affirmed that there is not one single voltage in the power net, but a range from the maximum voltage at the alternator or battery, to a minimum at the farthest electrical components. The different voltage levels and voltage drops at the test points show that the voltage across the terminals of a component depends on the connection to the power net. As a consequence, it is necessary to consider the influence of the wiring harness and the chassis ground for voltage stability analysis.

### 3.2 Multi level power nets

For many years, the introduction of multi-voltage systems has been discussed, as this would bring many benefits (Kassakian et al., 1996). The advantages of higher voltage power nets, e.g. the proposed 42 V system, were clearly shown in (Miller et al., 1999; Miller & Nicastri, 1998; Lukic & Emadi, 2002), but the automotive industry mainly stuck to the conventional reliable 12 V power net.
From the view of voltage stability analysis, multi level power nets are only two separated single level power nets coupled by an energy converter like a DC chopper converter. Therefore, without loss of generality, only a single voltage level is analyzed in this article. However, the components are analyzed for a wide range of voltages, so as to enable an eventual simulation of different types of power nets including multivoltage nets.

### 3.3 Power net test bench

To verify both the single components and the the whole system, a power net test bench has been built (Fig. 3b). This reference power net implements the schematic topology presented in Fig. 2. The primary goal of this power net is to achieve accurate measurement results. A further goal was to make the power net easily configurable, so that both real scenarios and synthetic test cases can easily be tested. In the following, the components necessary to emulate a realistic behavior of the power net in the test bench are described.
**Storage/Battery**: Although a battery simulation system has the advantage that the measurements and tests are easily repeatable and configurable (Schweighofer et al., 2003; Thanheiser et al., 2009), real batteries are used. Since the electrochemical processes in batteries are very complex, it is not easy to model, especially the transient processes, with the required accuracy. Several commercial battery sizes can be employed, ranging from compact to luxury class car's batteries ($C_{bat} = 60...90Ah$) in this test bench. The state of charge (SOC) can be precisely adjusted at a dedicated battery conditioning test bench in order to provide equal conditions in the experimental procedure.
**Source/Alternator**: The alternator is emulated by a physical model executed on a real time system. Input parameters are the battery's voltage, the engine speed and the alternator's start temperature. The real time system controls a regulated 300 A power supply unit.
**Wiring harness and chassis ground**: For a realistic analysis of the power net's behavior, the distributed structure must be reproduced as accurately as possible. In particular, the exact location of power distribution units, fuse boxes, and clamp control is important. Therefore, a real wiring harness of a luxury class vehicle is used.
The car body, which serves as return conductor, is also part of the power distribution network.

Especially if several loads are using the same grounding bolt, interactions may be caused. Here, a car body of the BMW 7 series is applied (Fig. 3b).

**Electric loads**: The structure of up to 80 loads is very complex in reality. Therefore, it is sufficient to consider only a representative selection to analyze voltage stability. While placing the electric loads, it is necessary to regard the power system's structure. This includes the choice of power distribution and fuse boxes, the wire's lengths and cross sections, as well as the number and location of grounding bolts. With an accurate placement, it is possible to analyze all real kinds of requests on the power net with considerably fewer loads. The ECUs in itself are not built in, but substituted by regulated electronic loads having high dynamics, which can demand arbitrary power profiles and emulate the behavior of the ECUs. In this way, the experimental studies are more flexible. For example, worst cases can easily be conducted, where multiple ECUs make power demands simultaneously.

**Control and measurement**: Both synthetic test cycles and measured power curves of the electric loads can be applied by the control software via analog control signals. A grid of about fifty voltage and current measurement points reports the state of the power net.

## 4. Modeling of the power net's components

To simulate the voltage, it is necessary to have stability models of the power net's components. The main components of the power net are the alternator, the battery, and the electrical loads. The wires of the wiring harness connect these components with each other. Furthermore, as presented in Fig. 2 the car body is part of the power distribution network. It is shown how these components can be modeled, with a particular focus on the wiring harness and the chassis ground modeling.

### 4.1 Alternator

The alternator delivers the electrical energy that is needed to supply the loads and to charge the battery. Usually, a claw-pole or Lundell alternator is employed in automotive power nets. The Lundell alternator itself is an electrically excited synchronous machine with a rectifier bridge. Via belt drive, the alternator is coupled to the combustion engine. As a consequence, the electrical energy output, and especially the current output $I_{alt}$, depends on the speed of the combustion engine. A voltage regulator modulates the excitation current $I_{exc}$ to obtain a voltage level $V_{alt}$ up to 15.5 V. Modern voltage regulators are equipped with diagnosis functions and are connected to one of the car's communication networks, e.g. the Local Interconnect Network (LIN). Fig. 5 shows a schematic of an alternator.

A suitable way to model the alternator for the voltage stability analysis is by means of electrical equivalent circuits. Examples of how such models can be derived are presented in (Bai et al., 2002; Lange et al., 2008).

### 4.2 Battery

For battery modeling, different approaches are possible. The most common are electrochemical models, mathematical models, and electrical models (Chen & Rincon-Mora, 2006). Depending on the purpose of the simulation, an adequate approach must be chosen. Because the I-V-characteristics are the most relevant physical phenomena to describe the battery in a voltage stability analysis of the automotive power net, an electrical model is the most suitable. These electrical models are equivalent circuits, consisting of voltage sources, resistors, and capacitors. (Ceraolo, 2000; Barsali & Ceraolo, 2002; Chen & Rincon-Mora, 2006) present detailed information on electrical battery models.

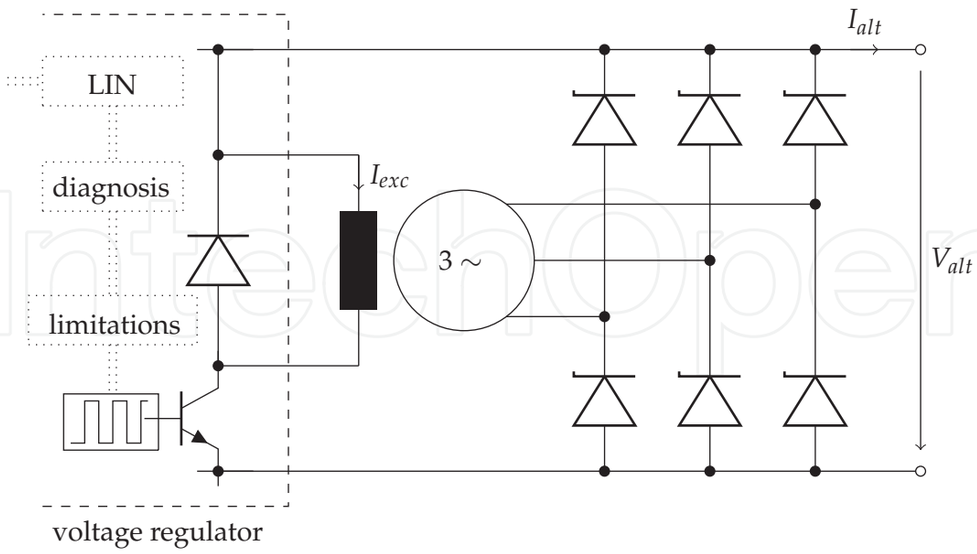


Fig. 5. Schematic of an automotive alternator. A voltage regulator controls the excitation of the electrical machine. The rectifier bridge converts the output of the electrical machine to DC.

A possible way to derive the parameters of such models is the method of impedance spectroscopy (Mauracher & Karden, 1997). Another method is to measure the voltage during discharge pulses and to fit the parameters based on the current and voltage curves (Bohlen, 2008).

### 4.3 Wiring harness

A common way to model transmission lines is by means of lumped circuit models (Paul, 1994). An example of a lumped-$\pi$ model of two wires above a ground plane is shown in Fig. 6. The derivation of the parameters of this model is presented.
To obtain simple but accurate models, it is discussed how the model can be simplified. To calculate the parameters, information on the geometrical arrangement of the single wires is needed. Fig. 7 shows an example of an arrangement of two wires above a ground plane.
The DC resistance of a wire with constant cross section $A$ and length $l$ can be calculated by

$$R_{dc} = \rho \frac{l}{A}, \tag{1}$$

where $\rho$ is the specific resistance of the conductor material. Additionally, it is common to use the per length resistance $R'$ in $\Omega/\mathrm{m}$.

$$R'_{dc} = \frac{\rho}{A} \tag{2}$$

Furthermore, the specific resistance $\rho$ is a function of the temperature and can be approximated by a Taylor series. For the temperature range that is relevant for the voltage analysis, this series can be stopped after the linear term:

$$\rho(\vartheta) = \rho_{\vartheta_{20}} \left(1 + \alpha_{\vartheta_{20}} \left(\vartheta - \vartheta_{20}\right)\right) \tag{3}$$

In (3) a reference temperature of 20°C was chosen. For copper $\alpha_{\vartheta_{20}}$ is 3.9 $\cdot 10^{-3}$ 1/K and $\rho_{\vartheta_{20}}$ is 0.0178 $\Omega$mm$^2$/m. This means a temperature rise of 25.8 K results in an increase in resistance of 10%.
The frequency $f$ must also be considered. Because of the skin effect, the AC resistance increases with frequency. The following formulas apply to solid, cylindrical conductors with circular cross section. The skin depth $\delta$ is the depth below the surface of the conductor at which the current density decays to $\frac{1}{e}$. The skin depth $\delta$ is given by

$$\delta = \frac{1}{\sqrt{\pi \mu \sigma f}} \tag{4}$$

$\mu$ is the permeability and $\sigma$ is the conductivity of the conductor material.
Usually, the AC resistance is calculated with the assumption that the current is uniformly distributed over an annulus at the wire surface of thickness equal to $\delta$ according to:

$$R'_{ac} = \frac{r^2}{2r\delta - \delta^2} R'_{dc} \approx \frac{r}{2\delta} R'_{dc} \text{ for } \delta \ll r \tag{5}$$

This approximation is suitable for high frequencies (Paul, 1994). To get an estimation of when the influence of the skin effect has to be considered, a more accurate calculation is based on a power series expansion for the Bessel functions (Simonyi, 1963). If the skin depth is more than 50% of the radius, the AC resistance can be approximated by

$$R'_{ac} = \left(1 + \frac{1}{3}\left(\frac{r}{2\delta}\right)^4\right) R'_{dc} \text{ for } \delta > \frac{r}{2}. \tag{6}$$

A method to calculate the skin effect in stranded wires is presented in (Gaba & Abou-Dakka, 1998), where $a_{geo}$ is the geometrical mean distance of the strands.

$$R'_{ac} = \sqrt{2\left(\frac{1 + (0{,}86\xi)^4}{2 + (0{,}86\xi)^4}\right)} \cdot R'_{dc} \quad \text{with} \quad \xi = \frac{a_{geo}}{\sqrt{2}\delta} \tag{7}$$

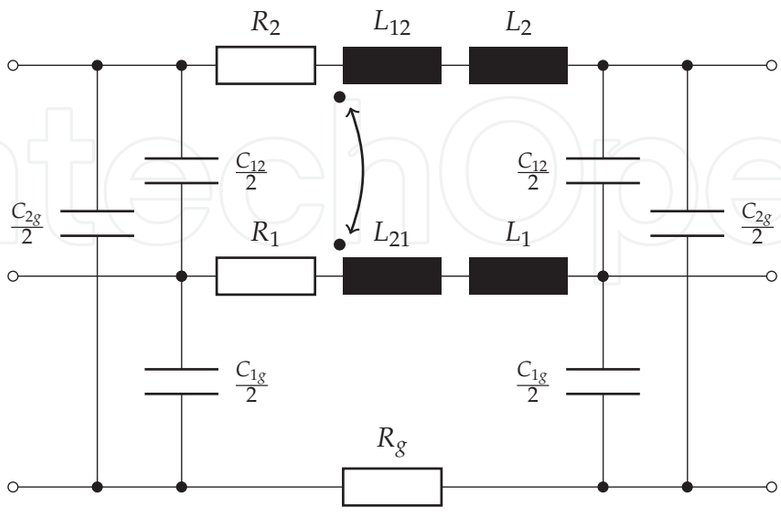


Fig. 6. Lumped-$\pi$ model for two wires above a ground plane (Smith et al., 1994). The model consists of 13 concentrated circuit elements.

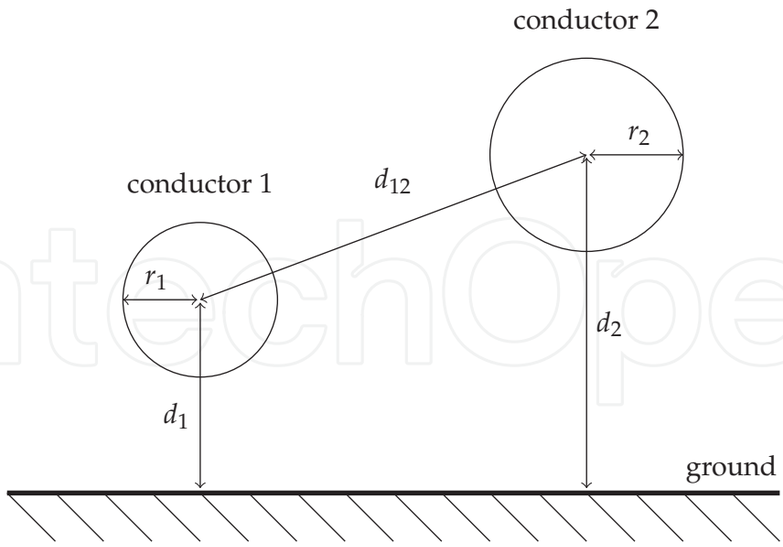


Fig. 7. Two conductors above a ground plane. Information on the geometrical dimensions of the arrangement is necessary to calculate the parameters of the lumped-$\pi$ model.

The per length self inductances $L_1'$ and $L_2'$ can be calculated according to:

$$L_1' = \frac{\mu}{2\pi} \ln\left(\frac{2d_1}{r_1}\right) \qquad L_2' = \frac{\mu}{2\pi} \ln\left(\frac{2d_2}{r_2}\right). \tag{8}$$

The per length mutual inductance $L_{12}'$ is:

$$L_{12}' = L_{21}' = \frac{\mu}{2\pi} \ln\left(\frac{D_{12}}{d_{12}}\right) \quad \text{with} \quad D_{12} = \sqrt{d_{12}^2 + 4d_1 d_2} \tag{9}$$

The per length capacitances can be derived by:

$$C_{1g}' = 2\pi\epsilon \frac{\ln\left(\frac{2d_2 d_{12}}{r_2 D_{12}}\right)}{\ln\left(\frac{2d_1}{r_1}\right)\ln\left(\frac{2d_2}{r_2}\right) - \ln^2\left(\frac{D_{12}}{d_{12}}\right)} \tag{10}$$

$$C_{2g}' = 2\pi\epsilon \frac{\ln\left(\frac{2d_1 d_{12}}{r_1 D_{12}}\right)}{\ln\left(\frac{2d_1}{r_1}\right)\ln\left(\frac{2d_2}{r_2}\right) - \ln^2\left(\frac{D_{12}}{d_{12}}\right)} \tag{11}$$

$$C_{12}' = 4\pi\epsilon \frac{\ln\left(\frac{D_{12}}{d_{12}}\right)}{\ln\left(\frac{2d_1}{r_1}\right)\ln\left(\frac{2d_2}{r_2}\right) - \ln^2\left(\frac{D_{12}}{d_{12}}\right)} \tag{12}$$

$\epsilon$ is the permittivity of the material surrounding the conductors.
Such calculations can be used to determine values of the parameters for typical wiring harness arrangements in automotive applications. Based on these guidelines, the influence of resistance, inductance, and capacitance on the voltage stability is evaluated in (Gehring et al., 2009) and modeling guidelines are derived.
The relevant frequency range for the voltage stability analysis is up to 10 kHz. In this range, the capacitance of the wires can be neglected. The per length capacitance is in the range of

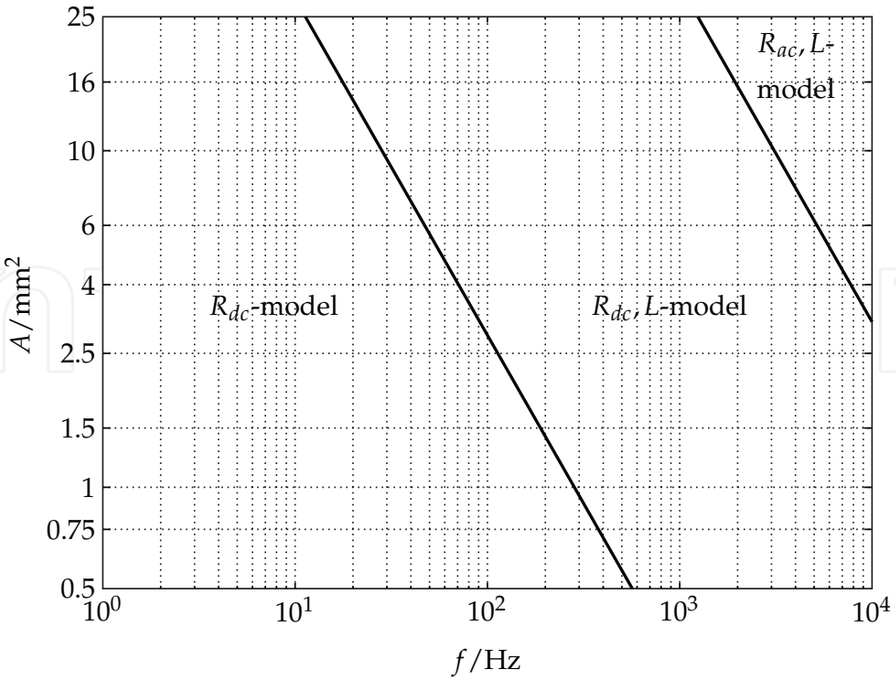


Fig. 8. Modeling guidelines: Based on the relevant frequency and the cross section of the wire, an adequate model can be selected.

picofarad. This means that for a frequency up to 10 kHz, $\frac{1}{\omega C'}$ is in the range of megohm. Compared to the per length resistance, which is in the range of milliohm, the influence of the capacitance is not relevant.

In contrast to this, the influence of the inductance must be considered (Gehring et al., 2009). The per length inductance is in the range of microhenry. This means that for a frequency up to 10 kHz $\omega L'$ is in the range of milliohm and comparable to the per length resistance.

In addition, the influence of the skin effect can become relevant even in the range of a few kilohertz.

Based on typical arrangements of automotive wiring harnesses, parameter values can be derived and used to define modeling guidelines. Fig. 8 shows these modeling guidelines.

Depending on the cross section and the frequency, a suitable model can be selected. For a cross section of 25 mm$^2$, a simple model with $R_{dc}$ can be used up to 10 Hz. For a cross section of 2.5 mm$^2$, the $R_{dc}$ model is appropriate up to a frequency of 100 Hz. If the cross section is 0.5 mm$^2$, the $R_{dc}$ model can be used up to a frequency of 560 Hz. The validation of these modeling guidelines can be found in (Gehring et al., 2009).

### 4.4 Fuses

Fuses protect the wires of the power net against overcurrent. The most common fuses in automotive power nets are blade fuses or bolt-on fuses with diffusion pill. Fig. 9 shows a schematic of these two different kinds of fuses.

Blade fuses usually have a rated current below 100 A. For higher currents, bolt-on fuses are used.

For the voltage stability analysis, the voltage drop across the fuses must be considered. Datasheets of fuse manufacturers offer resistance values that can be used to model fuses using electrical resistors. The behavior of fuses during opening is not part of the voltage stability

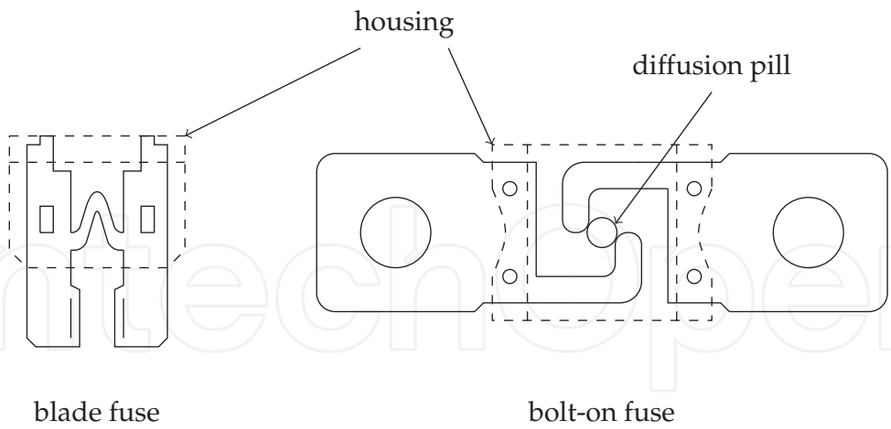


Fig. 9. For circuit protection, different kinds of fuses can be used. In the automotive wiring harness, the most common fuses are blade fuses or bolt-on fuses.

analysis presented in this article. For further information on this aspect see (Batchelor & Smith, 1999; 2001).

### 4.5 Chassis ground

As shown in Fig. 2. the car body is part of the power distribution network. As a consequence, it is necessary to analyze the voltage drop across the car body. Fig. 3a shows how the wires of the wiring harness are connected to the car body. The single wires are mounted to a bus bar. A screw nut connects the bus bar to a threaded bolt. The bolt itself is welded to the car body. Based on considerations known in the field of high voltage engineering (Velazquez & Mukhedkar, 1984), a method to calculate the resistance between two grounding bolts is presented. Furthermore, the calculation results are compared with measurements from a real car body.
As the car body is a complex structure, the following assumptions simplify the theoretical approach to calculate the resistance.

- the considerations are based on a stationary electric flow field
- the electric field close to the grounding bolts is radially symmetric
- the car body is regarded to be a plane sheet of steel with constant thickness and constant electrical conductivity

Fig. 10 shows the simplified system. Two grounding bolts, each with a radius of $r_1$, are welded to a flat sheet of steel. The steel thickness is $d$, the distance between the bolts is $r_2$.
Firstly, the field of one grounding bolt is regarded. The electric field $\vec{E}$ is related to the electric current density $\vec{J}$ through the conductivity $\sigma$:

$$\vec{J} = \sigma \vec{E} \tag{13}$$

The current $I$ is defined by the integral over a control surface $S$ over the current density $\vec{J}$.

$$I = \int_S \vec{J}\, d\vec{S} \tag{14}$$

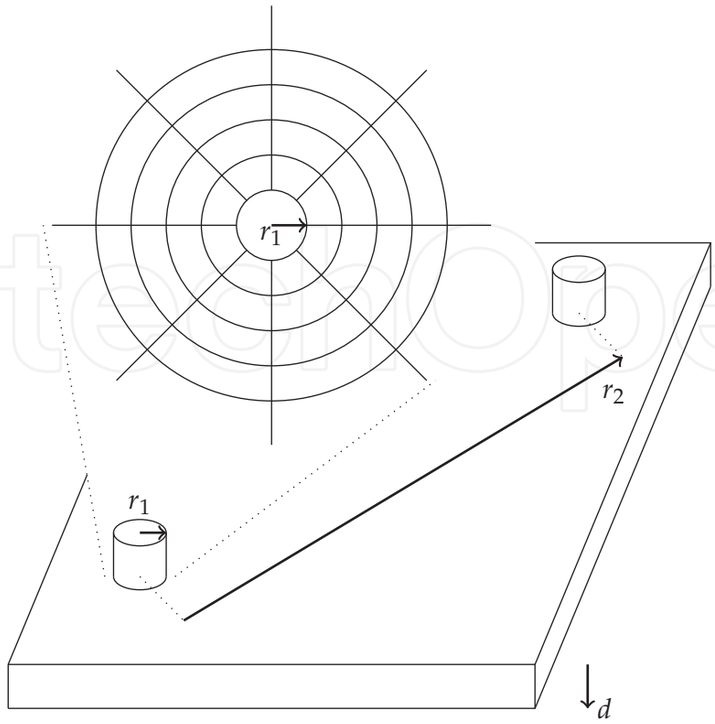


Fig. 10. The car body is regarded as a plane sheet of steel and it is assumed that the field close to the grounding bolts is radially symmetric.

In case of a grounding bolt, $S$ is the jacket of a cylinder with radius $r_1$, the radius of the grounding bolt, and the height $d$, the thickness of the sheet of steel. With (13) and (14) the electric field for $r > r_1$ becomes

$$\vec{E} = \frac{I}{2\pi\sigma r d}\,\vec{e}_r. \tag{15}$$

Because of the radially symmetric field, $\vec{E}$ only has a component in $r$-direction. By superposition of two fields, as described in (15), the voltage and resistance between two grounding bolts, respectively, can be calculated. The voltage between the two bolts is

$$V = \int_{r_1}^{r_2 - r_1} \vec{E}\, dr. \tag{16}$$

For the system of two grounding bolts as shown in Fig. 10, it follows that:

$$V = \frac{I}{2\pi\sigma d} \int_{r_1}^{r_2 - r_1} \frac{1}{r} + \frac{1}{r_2 - r}\, dr \tag{17}$$

With $V = RI$, the resistance between the two grounding bolts is:

$$R = \frac{1}{\pi\sigma d} \ln \frac{r_2 - r_1}{r_1} \tag{18}$$

As the bolts are welded to the car body, an offset $R_{welding}$ is added, to account for the influence of the welding quality. This offset is the sum of the resistances caused by the weld seam at each of the two grounding bolts. Hence, to calculate the resistance between two grounding

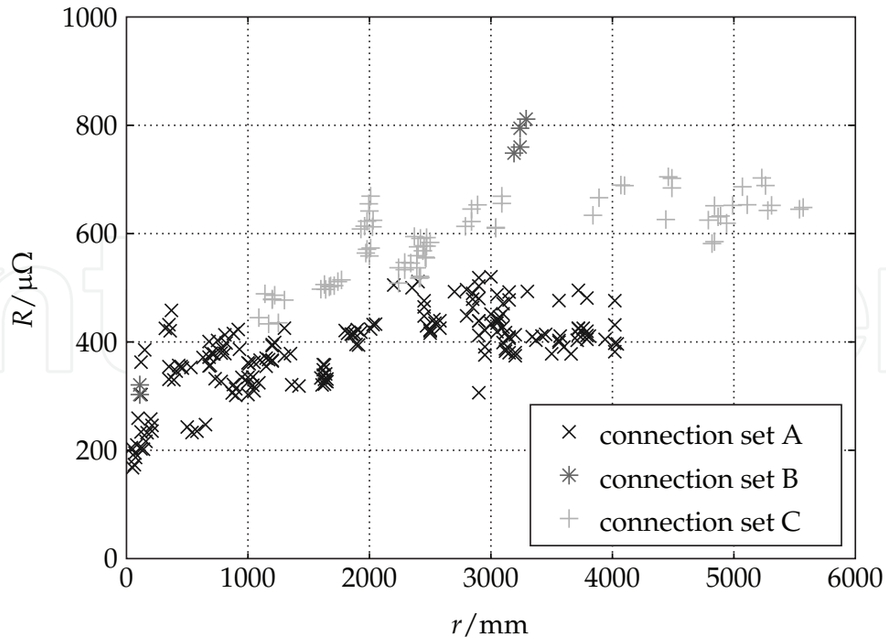


Fig. 11. Measured resistance between two grounding bolts. The resistance values are grouped according to the location of the grounding bolts.

bolts with radius $r_1$ set at a distance $r_2$ apart, the bolts being welded to a plane sheet of steel with thickness $d$ and conductivity $\sigma$, the following equation can be used:

$$R = R_{welding} + \frac{1}{\pi\sigma d} \ln \frac{r_2 - r_1}{r_1} \tag{19}$$

This theoretical approach was based on the assumption of a radially symmetric and stationary electric flow field. Furthermore, the car body was regarded as a plane sheet of steel with constant thickness. However, the car body is a complex structure of many metallic parts like girders and sheets of steel. Therefore, (19) has been compared with measurements on a real car body containing 23 grounding bolts. These 23 grounding bolts form a network with 253 possible connections. For each connection, a resistance value was measured by a four point measurement technique with a micro-ohm-meter. Fig. 11 shows the results.

The measured resistance values between two grounding bolts are grouped according to their location on the car body. One group represents connections of grounding bolts that are located in the passenger compartment or the trunk. These resistance values are marked as connection set A in Fig. 11. Another group represents the connections of grounding bolts that are located in the engine compartment. This is marked as connection set B in Fig. 11. The connection set C marks the connections with one grounding bolt located in the engine compartment and the other one in the passenger compartment or the trunk.

The measured resistance values can be used to parameterize the model derived in (19). This parameterization is shown in (Gehring et al., 2009). The influence of the weld seam $R_{welding}$ is between 85 and 160 $\mu\Omega$. If the grounding bolts are located close to each other on the same sheet of steel, than the parameter $d$ is the thickness of this sheet of steel.

Equation (19) is based on the assumption of a plane sheet of steel with constant thickness. The car body, however, is a complex structure of girders and many different sheets of steel that are welded together. As a consequence, an equivalent thickness $d'$ must be used for distant

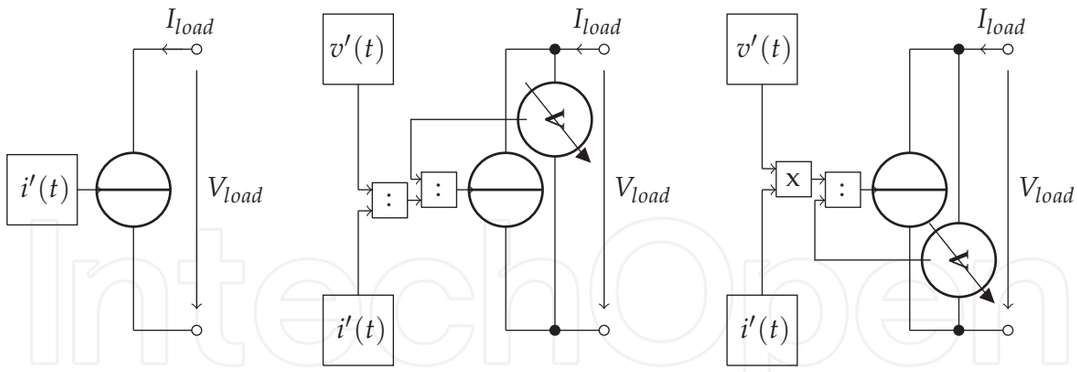


a) current based b) resistance based c) power based

Fig. 12. Structure of the loads' models. Loads are modeled by current-, voltage- or power-based sinks.

connections. The grouping in the connection sets A, B, and C results in three different values for $d'$.

An overview of these parameters is shown in Tab. 1. As the considerations are based on a stationary flow field, the proposed model can be used for the low frequencies that are relevant for the voltage stability analysis. For investigations of higher frequencies, for example considerations in the field of EMC, other approaches are more appropriate. An example can be found in (Smith et al., 1994).

### 4.6 Loads

Loads can be modeled as controlled current sinks. Input information for these sinks are data derived by measurements of the voltage and the current of each load. Depending on the characteristics of each load, the structure of the sinks is current-, resistance- or power-based. Fig. 12 shows the structure of the loads' models.

If, according to the modeling guidelines shown in Fig. 8, the inductance of the wires needs to be modeled, then loads should be modeled as controlled resistors. Furthermore, the input impedance of each load, caused by the capacitors and inductors of the EMI filters, should be accounted for the controlled resistor.

| Distance | Variable | Value |
|---|---|---|
| close connections | $R_{welding}$ | 85 μΩ ... 160 μΩ |
| | $d$ | 1.0 mm |
| distant connections | $R_{welding}$ | 85 μΩ ... 160 μΩ |
| | $d'$, passenger compartment & trunk (set A) | 0.60 mm ... 0.86 mm |
| | $d'$, engine compartment (set B) | 0.34 mm |
| | $d'$, mixed (set C) | 0.45 mm ... 0.61 mm |

Table 1. parameters of the grounding model according to (19)

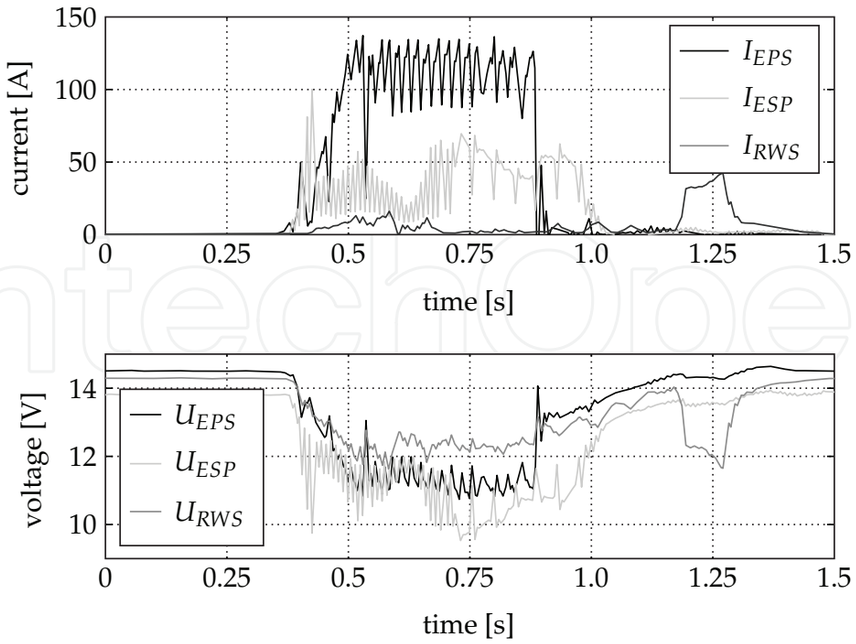


Fig. 13. Simulation example. During this driving scenario, different chassis control systems are active.

## 5. Simulation of the entire system

The models of the components form the basis for the simulation of the entire power net. With the simulation, different power net configurations with various loads and topologies can be put together and be evaluated in terms of voltage stability.

Fig. 13 shows a simulation example. The results of the simulation are compared with experimental results at the power net test bench. The first scenario which was investigated is based on measurements from a real car. In this scenario, the driver is driving at low speed and suddenly brakes to avoid hitting a pedestrian. The current and voltage curves of different loads were measured in the real car and used as inputs for the simulation and the test bench. Fig. 13 shows the current curves of three chassis control systems that are active during the driving scenario, and the resulting voltage curves at the terminals of these systems. The electrical power steering (EPS) reaches a maximum current of about 150 A, the rear wheel steering (RWS) a maximum current of 45 A. The electronic stability program (ESP) causes a current peak with a maximum of 90 A.

A comparison between the simulation results and the experimental results of the voltage curves of two of the three chassis control systems is shown in Fig. 14. $U_{EPS}$ sim. is the simulated voltage, $U_{EPS}$ me. is the measured voltage at the terminals of the electrical power steering. Analogously, $U_{ESP}$ sim. and $U_{ESP}$ me. are the simulated and measured voltages at the terminals, as produced by the electronic stability program. The deviations between the simulation and the experimental results are below 300 mV. Even at high current peaks, the accuracy of the simulated voltage compared to the measured voltage is in the range of 300 mV.

This means that the simulation can be used to investigate the voltage stability within the automotive power net. The derived simulation results represent the voltage behavior in an accurate manner.

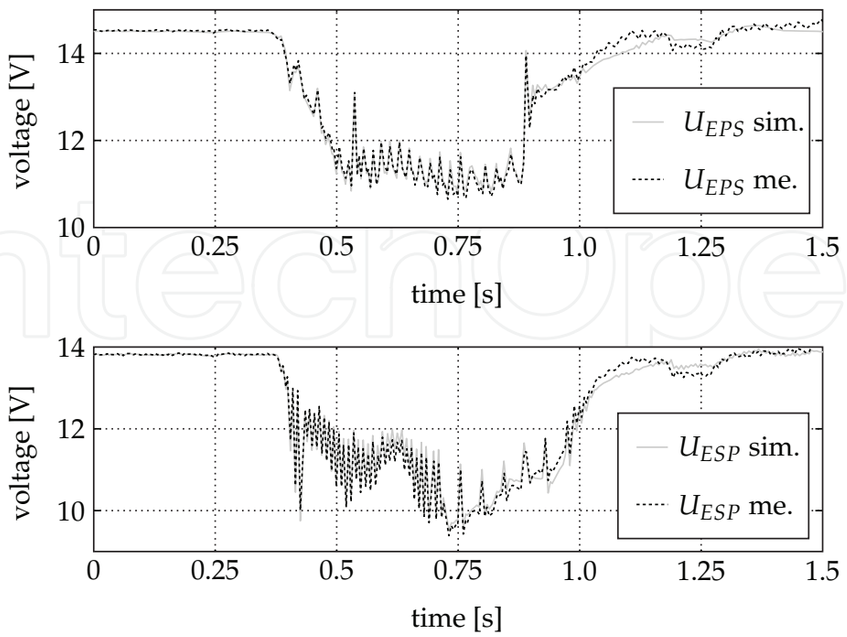


Fig. 14. Accuracy of the simulation at high voltage drops. The deviations are below 300 mV.

The advantage of using the simulation is that many different topologies of the power net can be evaluated virtually.
It must be considered, however, that the test bench is an additional and necessary tool to validate the simulation results.

## 6. Conclusion

Using the simulation models of section 4 and 5 or the power net test bench of section 3.3, it is possible to draw some conclusions about voltage stability issues and inherent risk for the electric components:

### 6.1 Critical situations

All investigations clearly show that there are mainly two critical cases:

– The electric power demand as a whole is high, so that the alternator is not able to completely supply the power net. Every additional load can generate critical (local) voltage drops.
– The activation of today's driver assistance systems causes extreme power rise times. More than 100 A in under 5 ms are a common scenario. The alternator cannot ramp up its power supply in the same period because its dynamics are limited to avoid feedback, which would potentially decrease the driving comfort.

To counteract these voltage drops, a dimensioning of the power net with thick wires and a big battery or more than one battery could be a solution. Another possibility is to develop an active and predictive power distribution management system that detects critical situations in advance. Then, suitable measures can be taken to pre-condition the electric power net. Some possible stabilizing measures are mentioned in (Kohler, Wagner, Gehring, Froeschl, Thanheiser, Bertram, Buecherl & Herzog, 2010).

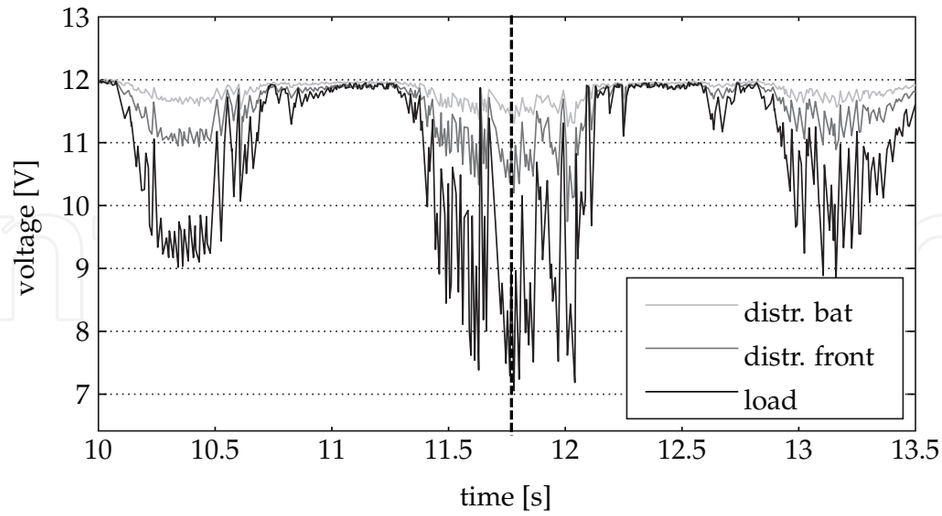


Fig. 15. Cut-out of a slalom driving maneuver with measurements at different places in the power net (distribution box at the battery and in the front and at the load) at the test bench. The vertical dashed line marks the time at which the analysis shown in Fig. 16 takes place.

### 6.2 Voltage drops in the wiring harness and car body

Besides the obvious voltage drops over the wiring harness at high currents, there are further drops at the distribution and fuse boxes. Likewise, there are significant losses on the return conductor, which have to be taken into account.

Fig. 15 presents the voltages, measured in a slalom driving maneuver at the power net test bench. In this case, as a result of the fast steering interventions, a few systems showing high peak power like electric power steering or dynamic stability control are simultaneously activated, and therefore particularly high power peaks occur in the whole system. The vertical dashed line in Fig. 15 marks the global load peak. Fig. 16 presents an analysis of the different voltages within the power distribution net at the moment in which the peak takes place.

Comparing the battery's and the load's terminals, it can be seen that the voltage decreased from 12.5 V to 7.1 V, which is a decline of above 40%. The main part of this decrease—4.4 V or 81%—is caused by the wiring harness, but a non-negligible part of 1.0 V or 19% is due to the return conductor.

### 6.3 Voltage stabilization

All the losses mentioned above depend on the installation location of the respective electric loads. Therefore, a power distribution management system should comprise both local and global levels. Today's systems that use a simple priority table and drop the less prioritized loads can be ineffective. The cut-off of a 40 A-load increases the voltage at the same distribution box by about 0.4 V. The influence on other places in the power net is only 0.2 V, or even less. For this reason, an optimized power distribution management system should account for the location of the power net's components and their interactions, specified in section 4 and 5.

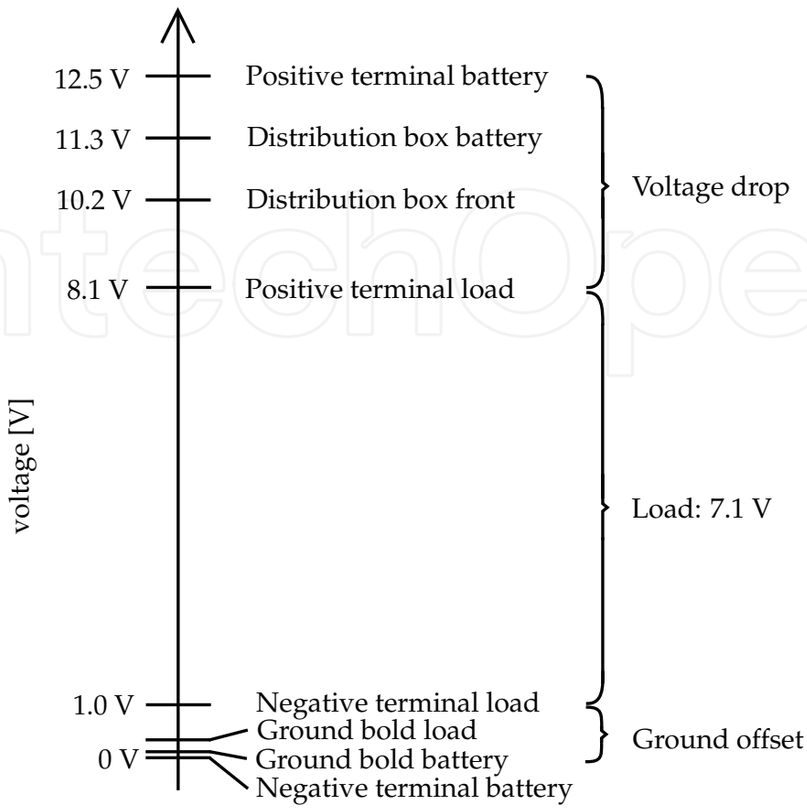


Fig. 16. Voltage at different measurement points at $t$ = 11.8 s of the slalom driving maneuver in Fig. 15. The resulting voltage at the terminals of the load is only 7.1 V.

## 7. Outlook

The analysis of voltage stability in various automotive power nets by simulation still requires further research, so as to gain a more detailed and profound understanding of various aspects of simulating voltage stability. As a contribution to the ongoing research, in this paper several aspects have been explored and understood, as reviewed below.

Firstly, with the method given in this paper, the wires can optimally be dimensioned. Further, one can inspect whether one wire is able to supply more than one component without having adverse reciprocal effects. For this reason, it will be possible to reduce both the weight and cost of the wiring harness.

Secondly, an optimization of the wiring harness' topology itself can be conducted. Conceptually, today's topologies are the same as they were in the 1960s; they have merely expanded with the increasing number of electric equipment components. Therefore, with the simulation methods outlined in this paper, alternative power net topologies should be tested: for example, alternative nets may include a collecting power bus, or a concept using distributed energy storage units. Furthermore, the influence of the packaging on the voltage stability becomes calculable. For instance, the assets and drawbacks of assembling the battery in the back of the vehicle can be investigated from a voltage stability point of view.

In spite of all topological improvements, voltage variation and drop can always occur. Therefore, all possible active measures should be taken to ensure safety and functionality, even

if a voltage drop should occur. For this purpose—finally—a power distribution management system should be developed, as was recommended in Kohler, Froeschl, Bertram, Buecherl & Herzog (2010). This system should detect critical situations in advance, and initiate stabilizing countermeasures. Using the knowledge of voltage stability analysis, measures can be tailored to the location of the voltage problem so as to guarantee maximum effectiveness.

## 8. References

Bai, H., Pekarek, S., Tichenor, J., Eversman, W., Buening, D., Holbrook, G., Hull, M., Krefta, R. & Shields, S. (2002). Analytical derivation of a coupled-circuit model of a claw-pole alternator with concentrated stator windings, *IEEE Transactions on Energy Conversion* Vol. 17(No. 1): 32 – 38.

Barsali, S. & Ceraolo, M. (2002). Dynamical models of lead-acid batteries: Implementation issues, *IEEE Transactions on Energy Conversion* Vol. 17(No. 1): 16 – 23.

Batchelor, A. & Smith, J. (1999). Time-current characteristic of miniature zinc-element electric fuses for automotive applications, *IEE Proceedings - Science, Measurement and Technology* Vol. 146(No. 4): 210–216.

Batchelor, A. & Smith, J. (2001). Extreme overcurrent analysis for the protection of automotive circuit components, *IEE Proceedings - Science, Measurement and Technology* Vol. 148(No. 2): 55–61.

Bohlen, O. (2008). *Impedance-based battery monitoring*, PhD thesis, Institute for Power Electronics and Electrical Drives - RWTH Aachen University.

Ceraolo, M. (2000). New dynamical models of leadacid batteries, *IEEE Transactions on Power Systems* Vol. 15(No. 4): 1184 – 1190.

Chen, M. & Rincon-Mora, G. (2006). Accurate electrical battery model capable of predicting runtime and i-v performance, *IEEE Transactions on Energy Conversion* Vol. 21(No. 2): 504 – 511.

Gaba, G. & Abou-Dakka, M. (1998). A simplified and accurate calculation of frequency dependence conductor impedance, *Proceedings of the* $8^{th}$ *Interantional Conference on Harmonics and Quality of Power*, IEEE, Athens, Greece, pp. 939 – 945.

Gehring, R., Froeschl, J., Kohler, T. & Herzog, H.-G. (2009). Modeling of the automotive 14 v power net for voltage stability analysis, *Proceedings of the Vehicle Power and Propulsion Conference, VPPC '09*, IEEE, Dearborn, USA, pp. 71– 77.

Gerke, T. & Petsch, C. (2006). Analysis of vehicle power supply systems using system simulation, *SAE 2006 World Congress & Exhibition, Detroit, MI, USA*.

Hillenbrand, M. & Muller-Glaser, K. (2009). An approach to supply simulations of the functional environment of ecus for hardware-in-the-loop test systems based on ee-architectures conform to autosar, *Rapid System Prototyping, 2009. RSP '09. IEEE/IFIP International Symposium on*, pp. 188 –195.

Kassakian, J., Wolf, H.-C., Miller, J. & Hurton, C. (1996). Automotive electrical systems circa 2005, *Spectrum, IEEE* 33(8): 22 –27.

Kiehne, H. A. H. (ed.) (2003). *Battery technology handbook*, Electrical and computer engineering ; 118, 2nd ed. edn, Dekker, New York. Includes bibliographical references and index.

Kohler, T., Froeschl, J., Bertram, C., Buecherl, D. & Herzog, H.-G. (2010). System approach of a predictive, cybernetic power distribution management, *The World Electric Vehicle Symposium and Exposition (EVS), Shenzhen, 2010*.

Kohler, T., Wagner, T., Gehring, R., Froeschl, J., Thanheiser, A., Bertram, C., Buecherl, D. & Herzog, H.-G. (2010). Experimental investigation on voltage stability in

vehicle power nets for power distribution management, *Vehicle Power and Propulsion Conference, 2010. VPPC '10. IEEE*.

Lange, E., van der Giet, M., Henrotte, F. & Hameyer, K. (2008). Circuit coupled simulation of a clawpole alternator by a temporary linearization of the 3dfe model, *Proceedings of the Interantional Conference on Electrical Machines*, IEEE, Vilamoura , Portugal, pp. 1 – 6.

Lukic, S. & Emadi, A. (2002). Performance analysis of automotive power systems: effects of power electronic intensive loads and electrically-assisted propulsion systems, *Vehicular Technology Conference, 2002. Proceedings. VTC 2002-Fall. 2002 IEEE 56th*, Vol. 3, pp. 1835 – 1839 vol.3.

Mauracher, P. & Karden, E. (1997). Dynamic modelling of lead/acid batteries using impedance spectroscopy for parameter identification, *Journal of Power Sources* Vol. 67(No. 1-2): 69 – 84.

Miller, J., Emadi, A., Rajarathnam, A. & Ehsani, M. (1999). Current status and future trends in more electric car power systems, *Vehicular Technology Conference, 1999 IEEE 49th*, Vol. 2, pp. 1380 –1384 vol.2.

Miller, J. & Nicastri, P. (1998). The next generation automotive electrical power system architecture: issues and challenges, *Digital Avionics Systems Conference, 1998. Proceedings., 17th DASC. The AIAA/IEEE/SAE*, Vol. 2, pp. I15/1 –I15/8 vol.2.

Paul, C. (1994). *Analysis of Multiconductor Transmission Lines*, John Wiley & Sons.

Polenov, D., Proebstle, H., Brosse, A., Domorazek, G. & Lutz, J. (2007). Integration of supercapacitors as transient energy buffer in automotive power nets, *Power Electronics and Applications, 2007 European Conference on*, pp. 1 –10.

Reif, K. (ed.) (2009). *Automobilelektronik: Eine Einfuehrung fuer Ingenieure*, Vieweg+Teubner Verlag / GWV Fachverlage GmbH, Wiesbaden, Wiesbaden. In: Springer-Online.

Schweighofer, B., Raab, K. & Brasseur, G. (2003). Modeling of high power automotive batteries by the use of an automated test system, *Instrumentation and Measurement, IEEE Transactions on* 52(4): 1087 – 1091.

Simonyi, K. (1963). *Foundations of Electrical Engineering*, Macmillan.

Smith, W., Paul, C., Savage, J., Das, S., Cooprider, A. & Frazier, R. (1994). Crosstalk modeling for automotive harnesses, *Proceedings of the IEEE Interantional Symposiumon Electromagnetic Compatibility*, IEEE, Chicago, USA, pp. 447 – 452.

Surewaard, E. & Thele, M. (2005). Modelica in automotive simulations – powernet voltage control during engine idle, *4th International Modelica Conference, 2005*, pp. 309 –318.

Thanheiser, A., Meyer, W., Buecherl, D. & Herzog, H.-G. (2009). Design and investigation of a modular battery simulator system, *Vehicle Power and Propulsion Conference, 2009. VPPC '09. IEEE*, pp. 1525 –1528.

Velazquez, R. & Mukhedkar, D. (1984). Analytical modelling of grounding electrodes transient behaviour, *IEEE Transactions on Power Apparatus and Systems* Vol. 103(No. 6): 1314–1322.

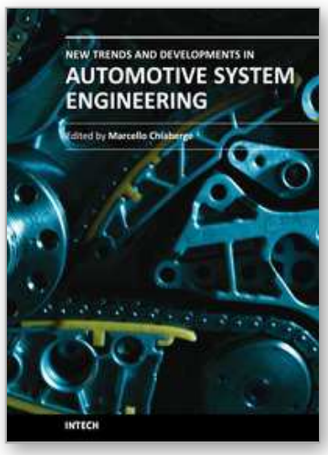


**New Trends and Developments in Automotive System Engineering**
Edited by Prof. Marcello Chiaberge

ISBN 978-953-307-517-4
Hard cover, 664 pages
**Publisher** InTech
**Published online** 08, January, 2011
**Published in print edition** January, 2011

In the last few years the automobile design process is required to become more responsible and responsibly related to environmental needs. Basing the automotive design not only on the appearance, the visual appearance of the vehicle needs to be thought together and deeply integrated with the â€œpowerâ€ developed by the engine. The purpose of this book is to try to present the new technologies development scenario, and not to give any indication about the direction that should be given to the research in this complex and multi-disciplinary challenging field.

**How to reference**
In order to correctly reference this scholarly work, feel free to copy and paste the following:

Tom P. Kohler, Rainer Gehring, Joachim Froeschl, Dominik Buecherl and Hans-Georg Herzog (2011). Voltage Stability Analysis of Automotive Power Nets based on Modeling and Experimental Results, New Trends and Developments in Automotive System Engineering, Prof. Marcello Chiaberge (Ed.), ISBN: 978-953-307-517-4, InTech, Available from: http://www.intechopen.com/books/new-trends-and-developments-in-automotive-system-engineering/voltage-stability-analysis-of-automotive-power-nets-based-on-modeling-and-experimental-results

INTECH
open science | open minds

**InTech Europe**
University Campus STeP Ri
Slavka Krautzeka 83/A
51000 Rijeka, Croatia
Phone: +385 (51) 770 447
Fax: +385 (51) 686 166
www.intechopen.com

**InTech China**
Unit 405, Office Block, Hotel Equatorial Shanghai
No.65, Yan An Road (West), Shanghai, 200040, China
中国上海市延安西路65号上海国际贵都大饭店办公楼405单元
Phone: +86-21-62489820
Fax: +86-21-62489821

IntechOpen